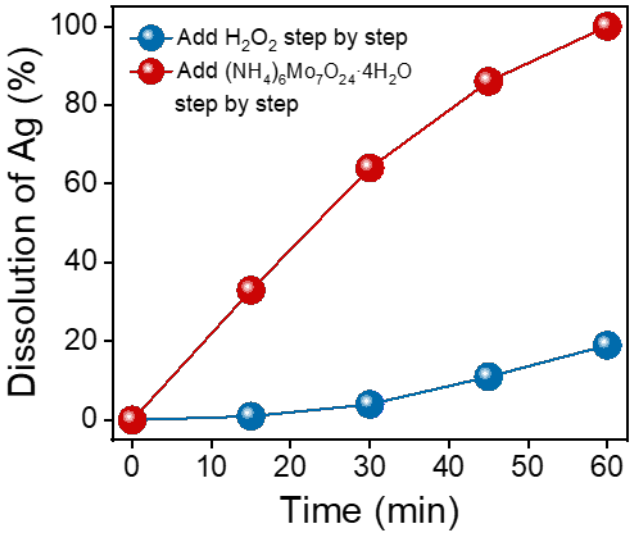


Figure S1. Effect of reagent addition mode on Ag leaching.

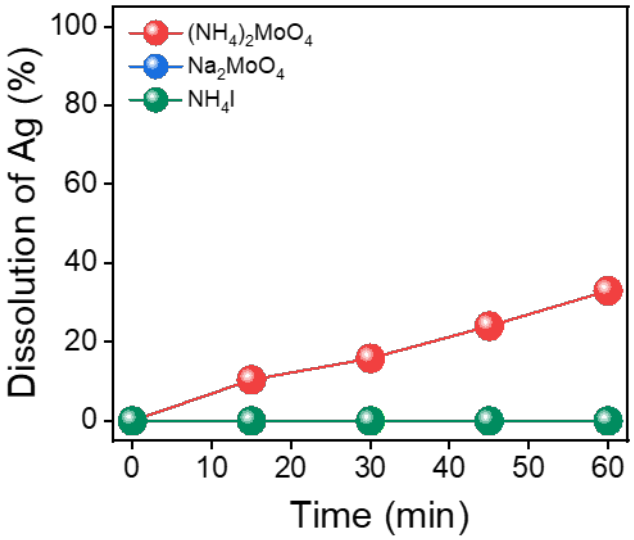


Figure S2. Effect of different molybdenum and ammonium sources on Ag leaching.

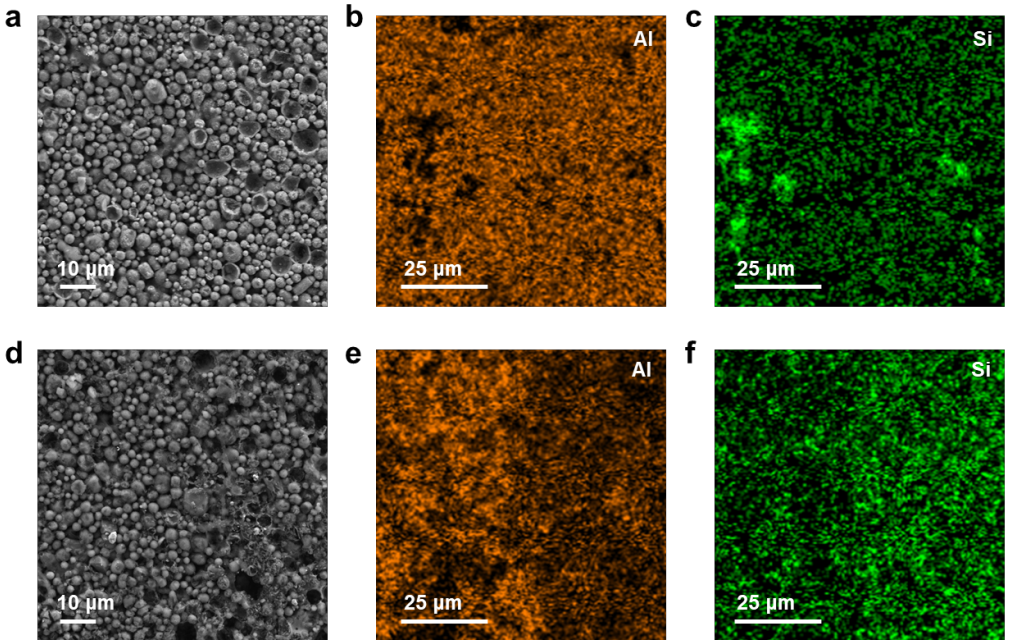


Figure S3. SEM image and corresponding EDS mapping of the back side of the PV panel: SEM before the reaction (a), Al mapping (b), and Si mapping (c); SEM after the reaction (d), Al mapping (e), and Si mapping (f).

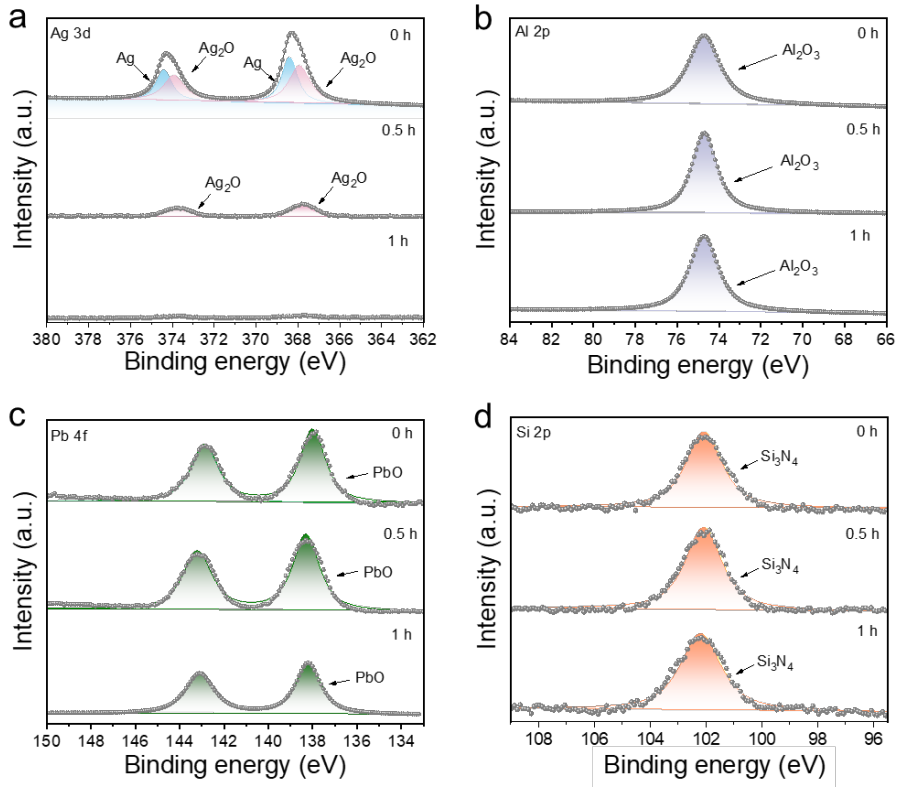


Figure S4. XPS spectra of the PV panel before and after leaching: (**a**) Ag 3*d*, (**b**) Al 2*p*, (**c**) Pb 4*f*, and (**d**) Si 2*p*.

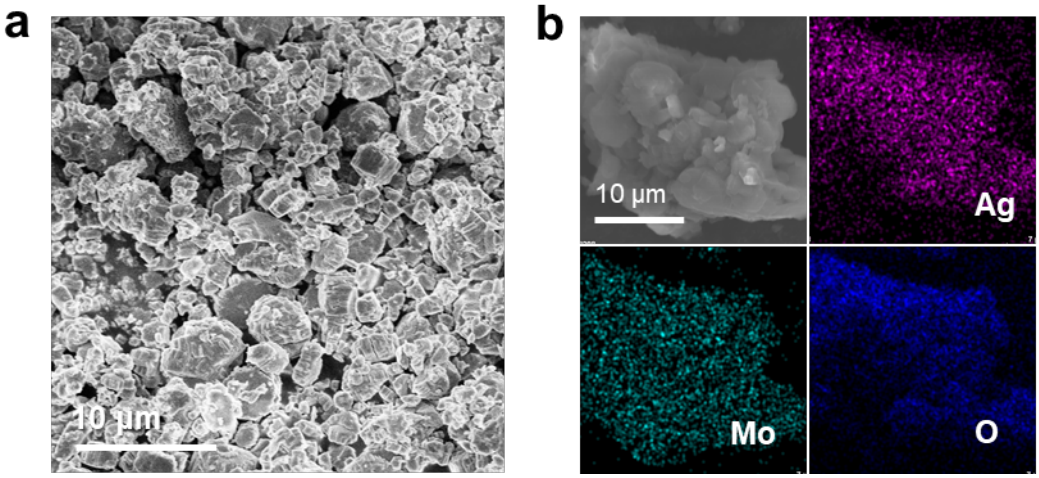


Figure S5. (**a**) SEM image and (**b**) EDS mapping of the recovered product.

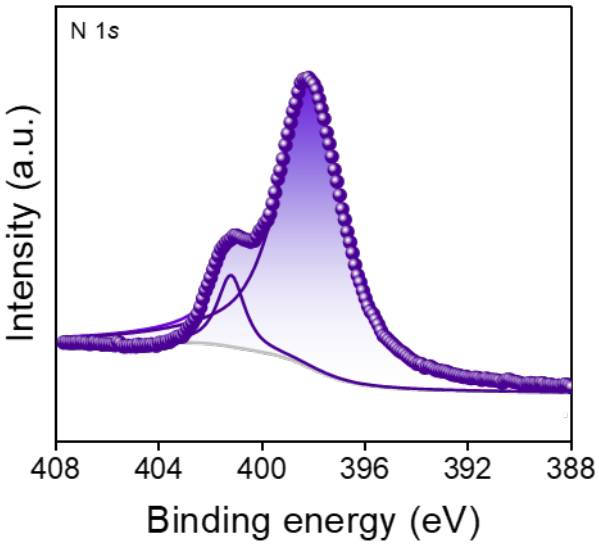


Figure S6. High-resolution N 1*s* XPS spectrum of the recovered product.

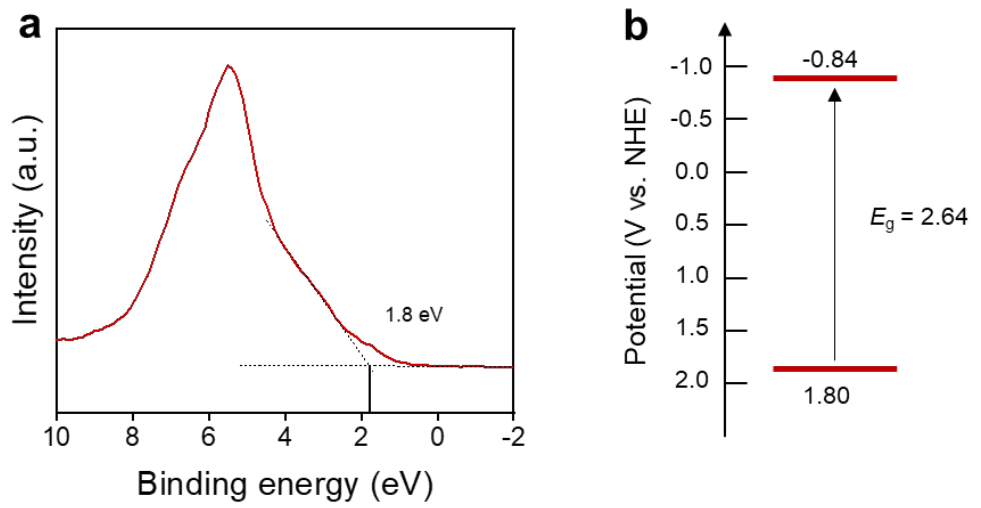


Figure S7. (**a**) UPS spectrum of the recovered $Ag_xMo_yO_z$. (**b**) Schematic energy band diagram of $Ag_xMo_yO_z$.

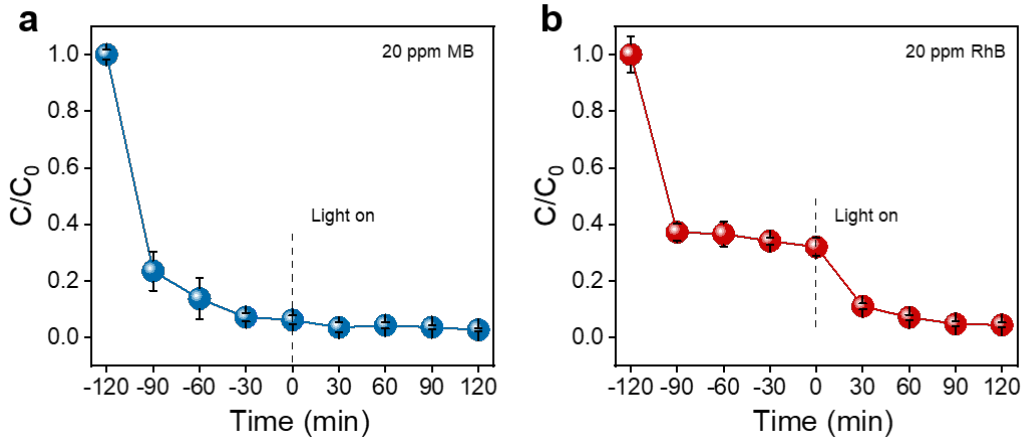


Figure S8. Adsorption performance and photocatalytic degradation of (**a**) MB and (**b**) RhB using $Ag_xMo_yO_z$.

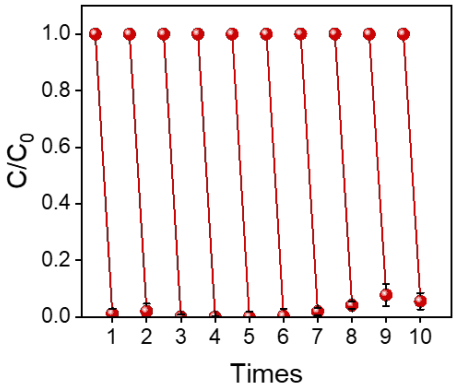


Figure S9. Cycling stability of the recovered $Ag_xMo_yO_z$ for photocatalytic degradation of RhB under visible-light irradiation.